Published in final edited form as:
Brain Res. 2009 November 17; 1298: 46–56. doi:10.1016/j.brainres.2009.08.073.

Nonphosphorylated neurofilament protein is expressed by scattered neurons in the vestibular and precerebellar brainstem

Joan S. Baizer, Ph.D.
Department of Physiology and Biophysics, 123 Sherman Hall, University at Buffalo, School of Medicine and Biomedical Sciences, Buffalo, NY 14214, 716-829-3096

Joan S. Baizer: baizer@buffalo.edu

Abstract

Vestibular information is essential for the control of posture, balance, and eye movements. The vestibular nerve projects to the four nuclei of the vestibular nuclear complex (VNC), as well as to several additional brainstem nuclei and the cerebellum. We have found that expression of the calcium-binding proteins calretinin (CR) and calbindin (CB), and the synthetic enzyme for nitric oxide synthase (nNOS) define subdivisions of the medial vestibular nucleus (MVe) and the nucleus prepositus (PrH), in cat, monkey, and human. We have asked if the pattern of expression of nonphosphorylated neurofilament protein (NPNFP) might define additional subdivisions of these or other nuclei that participate in vestibular function. We studied the distribution of cells immunoreactive to NPNFP in the brainstems of 5 cats and one squirrel monkey. Labeled cells were scattered throughout the four nuclei of the VNC, as well as in PrH, the reticular formation (RF) and the external cuneate nucleus. We used double-label immunofluorescence to visualize the distribution of these cells relative to other neurochemically defined subdivisions. NPNFP cells were excluded from the CR and CB regions of the MVe. In PrH, NPNFP and nNOS were not colocalized. Cells in the lateral vestibular nucleus and RF colocalized NPNFP and a marker for glutamatergic neurons. We also found that the cholinergic cells and axons of cranial nerve nuclei 3, 4, 6, 7,10 and 12 colocalize NPNFP. The data suggest that NPNFP is expressed by a subset of glutamatergic projection neurons of the vestibular brainstem. NPNFP may be a marker for those cells that are especially vulnerable to the effects of normal aging, neurological disease or disruption of sensory input.

INTRODUCTION

Vestibular information travels from the semicircular canals and otoliths to the brainstem via the eighth cranial nerve, and is distributed to the spinal (SpVe), medial (MeVe), lateral (LVe) and superior (SuVe) nuclei, which comprise the vestibular nuclear complex (VNC). However, analysis of vestibular signals is not restricted to the VNC. There are additional nuclei that receive direct vestibular afferents, for example the external cuneate nucleus, (ECu) and the subtrigeminal nucleus (Carleton and Carpenter, 1984; Kevetter et al., 2004; Korte, 1979). Other nuclei, for example for example the nucleus prepositus (PrH; Belknap and McCrea, 1988; McCrea and Horn, 2006) and cells of the reticular formation (RF;(Ladpli and Brodal, 1968)) receive vestibular signals from the VNC. We use the term “vestibular brainstem” to include the classic nuclei of the VNC as well as other nuclei that receive vestibular information.

Many anatomical studies suggest that the internal organization of the nuclei of the vestibular brainstem is complex. Afferents may be distributed to multiple nuclei but only to restricted regions of each, similarly, some efferents arise from restricted regions of multiple nuclei (references and discussion in Baizer and Baker, 2005; Baizer and Baker, 2006a). These different anatomically-defined regions are not seen in cell or fiber-stained sections. We have, however, begun to find neurochemical correlates of this organizational complexity. There are two neurochemically-defined subregions of the MVe, one characterized by the presence of calretinin (CR) in cells and fibers, the other by dense calbindin (CB) immunoreactivity in axons. These subdivisions are present in cats, monkeys and humans (Baizer et al., 2006; Baizer and Baker, 2005; Baizer and Baker, 2006a; Baizer and Baker, 2006b). In PrH of cats and monkeys, we found a cell column defined by immunoreactivity to the synthetic enzyme for nitric oxide, nitric oxide synthase, nNOS (nNOS; Baizer and Baker, 2006b).

Expression of nonphosphorylated neurofilament protein (NPNFP), has shown functional subdivisions in the visual cortex (Hof and Morrison, 1995; Van Der Gucht et al., 2006; Van der Gucht et al., 2007) and labels specific cell populations in the lateral geniculate nucleus (Bickford et al., 1998) and superior colliculus (Fuentes-Santamaria et al., 2006). We have asked if its expression in vestibular brainstem might visualize either additional compartments or mark specific cell populations.

A brief report of some of these results has been presented as an abstract (Baizer and Baker, 2004).

RESULTS

We examined the expression of NPNFP in the four nuclei of the VNC, as well as PrH, ECu, the reticular formation (RF), the supragenicuate nucleus (SGe) and several cranial nerve nuclei. In the vestibular brainstem the immunolabel was found primarily in cell somas and dendrites; cell nuclei were never labeled. In the cranial nerve nuclei axons were also labeled. At the spacing of sections we examined, there were no consistent clusters or subregions defined by the labeled cells in the vestibular brainstem; the staining pattern in each nucleus was consistent throughout its rostro-caudal extent. However, the frequency of the labeled cells differed in different structures.

SpVe. Figure1 A shows NPNFP staining in the SpVe. The SpVe is crossed by stained processes running at all orientations. There are scattered large, stained multipolar cells (examples at arrow); cell bodies vary in shape with oval, polygonal and triangular examples seen. Figure 1B shows a higher magnification image of staining in the SpVe at the level of the dorsal region sometimes termed the paravestibular nucleus, PaVe (Paxinos et al., 2000, but not Berman, 1968). In the PaVe, staining is darker than in the more ventral SpVe (Fig. 1B); cells and processes are stained. The arrow shows a stained large cell in the SpVe with several primary dendrites; several other stained cells are visible. The axons that run through the SpVe and are cut in cross-section in this plane of section are not stained (Fig. 1B, arrowhead). Figure 1C shows a higher magnification image of a stained large cell with a triangular cell body in the SpVe with staining of the soma and of proximal dendrites that can be followed for over 200 μm (Fig. 2C, arrowhead). **MVe**. Figure 1A shows that there stained processes running at all orientations over the MVe. There were also scattered stained cells, but these were less frequently encountered than in the SpVe. Figure 2 (A, B, arrows) shows two examples of stained cells in the MVe. Figure 2A shows a large neuron with an irregularly shaped soma, and Figure 2B a cell with a pear-shaped soma. We also used double-label immunofluorescence to ask how the NPNFP-immunoreactive (ir) cells were arranged relative to the previously-described regions defined by CR and CB immunoreactivity (Baizer and Baker, 2005). Figure 2 C, D and E show immunofluorescence images of sections stained for both NPNFP and CR.

The white arrows in Figure 2C indicate the location of the CR area under the ventricle. Figure 2D shows that NPNFP-stained cells (example at arrow) in this section are located ventral to the CR area. We did not see any cells that colocalized both NPNFP and CR. The relation between the two populations is also seen in the merged image in Figure 2E. Figure 2F (white arrows) shows the region of dense CB fiber staining that is seen at the border of PrH and MVe. Figure 2G, arrow, shows an NPNFP-ir cell in this section that is in the MVe lateral to the fiber patch. Figure 2H shows the relation between the NPNFP cells and the CB fiber patch. On all sections examined, the NPNFP–ir cells were located outside the region of dense CB fiber label. **LVe**. Figure 3 A shows the many large labeled cells in the LVe; this nucleus has the highest density of stained cells of any of the nuclei of the VNC. The stained cells have irregularly shaped somas. The fibers of the vestibular nerve itself (8Ve) were not stained (Fig. 3B). Figure 3 B, C, D, shows images of three cells in the LVe that are labeled with the NPNFP antibody as well as by an antibody to a glutamate transporter. The two proteins were colocalized in these cells and in all cells in the LVe on the sections we examined. **SuVe**. There are also many stained cells in the SuVe; Figure 4A shows the stained cells with a variety of soma shapes. This figure also illustrates the higher density of stained cells in the SuVe than in the neighboring MVe. There are also stained cells and thick stained processes oriented parallel to the ventricle in the region just dorsal to the genu of the seventh nerve, the supragenicular nucleus SGe, (Fig. 4B, arrowhead shows a stained cell). **PrH**. As in the SpVe and MVe, there are labeled processes at all orientations throughout PrH (Fig. 5A) and a few stained large neurons (Fig. 5A, example at arrow). We asked what the relation between the NPNFP cells was to the nNOS cell column in PrH (Baizer and Baker, 2006b). Figure 5B,C, D shows three images of a section that was double-labeled for NPNFP and nNOS. Figure 5C shows an NPNFP labeled cell (arrowhead) and labeled processes and puncta in PrH. Figure 5B shows the nNOS cell cluster containing many labeled cells (examples at arrows). Figure 5D shows that the NPNFP-labeled cell is in the middle of the nNOS cells, but it does colocalize nNOS. **ECu**. There are also scattered stained cells in the ECu, with oval, elongated or irregular cell bodies (Fig.6A). We have seen several other neurochemically-defined cell populations in the ECu, including cells expressing CR and cells expressing nNOS (unpublished observations). Figure 6 (B, C, D) shows three images from a section through the ECu labeled for both NPNFP and nNOS. Figure 6C shows two NPNFP cells, and Figure 5D shows a cell labeled for nNOS. Figure 6B suggests that these are two independent populations. **RF**. There are scattered, very large multipolar NPNFP stained cells in the reticular formation. Figure 7A shows two examples, and Figure 7B, C shows that these two cells colocalize NPNFP and a glutamate transporter. **Cranial nerve nuclei 3, 4, 6, 7,10, 12**. In the course of analyzing the vestibular brainstem, we saw that cells and axons of cranial nerve nuclei were darkly labeled for NPNFP. Figure 8A shows NPNFP label of axons in the genu of the seventh nerve, and Figure 8B shows that cells in the hypoglossal nucleus colocalize ChAT, the synthetic enzyme for acetylcholine, and NPNFP.

Squirrel Monkey

A similar distribution of NPNFP- labeled cells and processes was found in the squirrel monkey vestibular brainstem (data not shown).

DISCUSSION

As a component of our ongoing investigation of the neurochemical organization of the vestibular brainstem, we have analyzed the distribution of cells that express nonphosphorylated neurofilament protein, NPNFP. These cells are found throughout the vestibular brainstem, but at different densities in different nuclei. This is in contrast to the geographical segregation of the cells in the MVe expressing the calcium-binding protein CR (Baizer and Baker, 2005b; Baizer and Baker, 2006a; Baizer and Broussard, 2009), and the cells in PrH that express nNOS.

NPNFP, cytoarchitectonics and chemoarchitectonics

Brodal has described the many different cell types of the VNC. How do our findings relate to his descriptions? The large labeled cells in the SpVe cells seem to correspond to the population of large multipolar neurons described by Brodal (Brodal and Pompeiano, 1957; 1962). For the other three nuclei, the labeled cells vary in soma size and shape, and seem to represent a subset of all different cell types described by Brodal. The MVe is sometimes divided into parvocellular (dorsal) and magnocellular (ventral) subdivisions (Epema et al., 1988; Paxinos and Huang, 1995; Paxinos et al., 1999) although these subdivisions have not been noted in the cat (Berman, 1968; Brodal and Pompeiano, 1957). The NPNFP cells in the MVe do not seem to be preferentially located in either region. Anteriorly, the SGe has sometimes been considered a rostral extension of PrH (Berman, 1968); the very different staining patterns in the two regions, however, argue for their status as separate nuclei. The nucleus PrH also includes a number of different cell types (McCrea and Horn, 2006); the NPNFP labeled population most closely resembles the “multidendritic” cells.

Our double-label immunofluorescence data are consistent with the idea that the NPNFP of the vestibular brainstem do not colocalize either CR or nNOS, and are glutamatergic. We cannot, however, rule out the possibility that NPNFP is also expressed by some cholinergic cells in the vestibular brainstem. First, NPNFP can be expressed by cholinergic neurons, since the cells of the cranial nerve nuclei express both NPNFP and ChAT. Second, multiple studies have shown that there is a population of cells immunoreactive to ChAT in the vestibular brainstem, although there is considerable disagreement about their distribution (Barmack et al., 1992a; Barmack et al., 1992b; Ikeda et al., 1992; Jones and Beaudet, 1987; Kimura et al., 1981; Motts et al., 2008; Satoh et al., 1983). Some of this disagreement may reflect differences among species (Motts et al., 2008, see Table 1), some may reflect technical differences among laboratories.

Connections

NPNFP cells in vestibular brainstem most likely represent a subset of glutamatergic projection neurons. Since the NPNFP labeled cells are relatively large, they can support larger diameter axons and long projections, suggesting that they contribute to projections to distant targets. The major targets of projections from the VNC are the spinal cord, cranial nerve nuclei 3, 4, and 6, the cerebellum, the inferior olive, PrH, the reticular formation, and the contralateral vestibular brainstem (Bankoul and Neuhuber, 1992; Bankoul et al., 1995; Barmack, 2003, review; Brodal, 1962; Brodal and Brodal, 1983; Buttner-Ennever, 1992 review; Gerrits et al., 1985; Hoddevik et al., 1991; Holstege and Kuypers, 1982; Holstein, 2000b; Kotchabhakdi et al., 1978; Kushiro et al., 2008; Langer et al., 1985; Minor et al., 1990; Peterson et al., 1978). While conclusive determination of the connections of the NPNFP cells would require combining injections of retrograde fluorescent tracers with immunohistochemistry, it is likely that NPNFP cells in the SpVe, MVe, LVe and RF contribute to vestibulospinal or reticulospinal projections (Brodal, 1962; Büttner-Ennever, 1992). For the MVe, however, NPNFP cells must represent only a small subset of vestibulospinal neurons, since electrophysiological and anatomical data suggest that the latter are more numerous (Bankoul and Neuhuber, 1992; Kushiro et al., 2008; Peterson et al., 1978). NPNFP cells must participate in other projections, however. Neither the PrH nor the SuVe contribute to vestibulospinal projections (review in Büttner-Ennever, 1992) but do project to cranial nerve nuclei 6, and 3 and 4, respectively (Büttner-Ennever, 1992). Another possible destination of axons of NPNFP cells in the VNC, PrH and the ECu is the cerebellum (Belknap and McCrea, 1988; Büttner-Ennever, 1992; Gerrits et al., 1985; Langer et al., 1985; Somana and Walberg, 1980).

NPNFP in the brainstem of other species

The distribution of labeled cells that we describe in cat and squirrel monkey is similar to results in the rat (Paxinos et al., 1999). Cells stained with the SMI32 antibody are shown in the ECu (Fig. 186), MVe and SpVe (Fig. 166, 138), PrH (Fig. 138), the LVe (Fig. 124), and the SuVe (Fig. 117). However, fibers of the seventh and eighth nerve are stained (Figs. 96; 110). Cells in the trochlear nucleus (Fig. 40) and oculomotor nucleus (Fig. 26) were labeled, whereas cells in the abducens (Fig. 96) did not appear to be. Similar results were reported for the short-beaked echidna (Ashwell et al., 2007). The data suggest that expression of this protein in vestibular brainstem is well-conserved across mammalian species, with some possible species differences.

Neurofilament protein, aging and disease

Loss of control of balance and falls are a major medical concern for the elderly (discussion and references in Ashley et al., 1977; Blaszczyk et al., 2000; Bloem et al., 2003; Kalchthaler et al., 1978; McGibbon, 2003). One idea is that there is a loss of vestibular compensation with age (Drago et al., 1996; Giardino et al., 2002; Heskin-Sweezie et al., 2009; Paige, 1992; Tian et al., 2001). This in turn would impair the ability of the system to adapt to a decrease in vestibular input, which also can occur with aging (Johnsson, 1971; Paige, 1992). One factor contributing to the loss of plasticity may be the loss of cells in the VNC (Alvarez et al., 1998; Alvarez et al., 2000). Several lines of evidence suggest that cells expressing NPNFP may be among the vulnerable population. Changes in neurofilament proteins in motor system disorders like amyotrophic lateral sclerosis (review in Xiao et al., 2006), motoneuron disease (Xu et al., 1993) and in various brainstem cell populations in normal aging are well-documented (Zhang et al., 2000). Cortical cells expressing NPNFP are lost in Alzheimer's disease (Bussiere et al., 2003; Hof et al., 1990; Hof and Morrison, 1990). Cells in the vestibular brainstem expressing NPNFP may also be sensitive to the disruption of sensory input, as are NPNFP cells in the visual system (Bickford et al., 1998; Duffy and Livingstone, 2005). Brainstem cells expressing NPNFP may thus undergo degenerative changes with normal and pathological aging, with loss of vestibular input, as well as with different neurological disorders. The loss of this population, then, would be expected to affect several different aspects of vestibulomotor function.

Experimental Procedures

Animals and tissue preparation

We studied brainstems of four cats and one squirrel monkey. All animal experiments were conducted according to the Principles of Laboratory Animal Care set forth by the National Institutes of Health in the Guide for Care and Use of Laboratory Animals. Procedures were approved by the Institutional Animal Care and Use Committee at Northwestern University. These animals had been used in anatomical and physiological studies of the vestibular system (Baizer and Baker, 2005; Baizer and Baker, 2006b; Sekerkova et al., 2005). At the conclusion of those physiological experiments, the animals were deeply anesthetized with Sodium Pentobarbital and then perfused through the aorta with 0.9% saline followed by 4% paraformaldehyde in phosphate buffered saline (PBS). The brains were removed, and the brainstems and cerebella were dissected away. The tissue blocks were cryoprotected in graded concentrations of sucrose in PBS (10%, 20% and 30%), quick frozen in −70° C isopentane or a frozen solution of 30% ethylene glycol and 30% glycerol in phosphate buffer (PB), and stored in a −70° C freezer. Frozen frontal sections (40 or 50 μm thick) were cut on an American Optical sliding microtome and stored at −20° C in tissue culture dishes (3–5 sections/well) in a cryoprotection solution of 30% ethylene glycol and 30% glycerol in PB.

Immunohistochemistry

Initially, sections about 1 mm apart were processed for immunoreactivity to NPNFP using standard immunohistochemical techniques and the "SMI-32" antibody (Sternberger Monoclonals, Inc. and Covance). Based on the initial analysis of these sections, selected sections were processed for double-label immunofluorescence. Procedures for single label immunohistochemistry were as previously described (Baizer and Baker, 2005; Baizer and Baker, 2006a; Baizer and Baker, 2006b). Briefly, sections were removed from the cryoprotectant, rinsed in PBS (all rinses were 3×10 min each), and incubated in a solution of PBS or PBS with 5% nonfat dry milk, 0.3 %Triton-X100, 1.5% normal serum, and the primary antibody overnight on a tissue shaker at 4° C. Sections were then rinsed in PBS and incubated in an anti-mouse IgG biotinylated secondary antibody (Vectakit, Vector Laboratories) in PBS with 0.3 % Triton X-100 and 1.5 % normal serum for one hour at room temperature on a shaker, rinsed again, and incubated for one hour in the Vector "ABC" solution on a rocker at room temperature. Immunoreactivity was visualized by incubating sections in 3,3'-diaminobenzidine (DAB, Sigma) with .0015-.003% H_2O_2 in 0.01M PBS or with a glucose-oxidase modification of that protocol (Shu et al., 1988). There was no immunostaining on control sections from each case that were processed with the primary antibody omitted. Sections were then mounted onto gelled glass slides, dehydrated in graded alcohol concentrations, cleared in Histosol (National Diagnostics) and coverslipped with Permount (Fisher Scientific). For the double-label immunofluorescence, sections were rinsed, blocked and then incubated with two primary antibodies simultaneously overnight on a shaker at 4° C. They were then rinsed and incubated with two secondary fluorescent antibodies (Alexa donkey anti-mouse 488, Alexa donkey anti-rabbit 594 or Alexa donkey antigoat, 568, all at 2.5 μg/ml), rinsed, mounted on gelled slides and coverslipped with Vectashield Hard Set mounting medium (Vector Laboratories).

Antibodies and specificity

NPNFP, "SMI32," Sternberger Monoclonals, Inc.; Covance, mouse. This antibody recognizes a nonphosphorylated epitope on the168 (M) and 200 kDa (H) neurofilament subunits (Sternberger and Sternberger, 1983) of most mammalian species and stains somas, dendrites and some thick axons (manufacturer's data). It lacks cross reactivity to microtubule associated protein or to Alzheimer's neurofibrillary tangles (Ksiezak-Reding et al., 1987; Lee et al., 1988). It was used at a dilution of 1:2000 for DAB/GO visualization and 1:1000 for immunofluorescence.

nNOS, nitric oxide synthase, Cayman Laboratories, 160870, rabbit polyclonal, 1:200. This antibody was raised against a peptide corresponding to amino acids 1422–1433 of human nNOS. It recognizes a peptide of 155–160 kDa on Western blot (manufacturer's data).

Glutamate transporter, Chemicon Ab 1520, goat, 1:1000. The antigen was the synthetic peptide from the carboxy-terminus of the cloned rat neuronal glutamate transporter, EAAC1.

Calretinin, Chemicon AB5054, rabbit, polyclonal,1:1000. The antibody was raised against recombinant rat calretinin, a 29 kDa protein, and recognizes both bound and free calretinin (data from manufacturer).

Calbindin D-28K, Chemicon, AB1778, affinity purified, rabbit polyclonal, 1:1000. The immunogen was recombinant CB. The antibody recognizes a 28kDa protein on immunoblot (manufacturer's data).

ChAT, Chemicon AB143, rabbit polyclonal. The immunogen was human placental enzyme.

Data analysis and photography

We used the Berman (1968) atlas of the cat brainstem to determine the approximate stereotaxic anterior-posterior (A-P) levels of the cat sections, and the atlas of Emmers and Akert (1963) for the squirrel monkey sections. We used three sources for terminology and abbreviations (Büttner-Ennever and Gerrits, 2004; Koutcherov et al., 2004; Paxinos and Huang, 1995). We examined the sections with a Leitz Dialux 20 light microscope. For the photomicrographs, digital images were captured using a SPOT Insight Color Mosaic camera (1200 × 1600 pixels) mounted on that microscope. Brightness and contrast of images were adjusted and plates composed with Adobe Photoshop software. For each image from the cat brainstem we indicate the approximate stereotaxic level relative to earbar 0 based on the pictures in the atlas of Berman (1968) at the top of the panel. Images of fluorescent sections were captured with a Zeiss Axioimager Z1 Axiophot wide-field fluorescence microscope. Brightness and contrast of images were adjusted with Zeiss Axiovision software. The figures were then assembled with Adobe Photoshop software.

Acknowledgements

Supported by a subcontract to JSB from NIH grant RO1 EY07342, James F. Baker, PI and by the Department of Physiology and Biophysics, University at Buffalo. We are grateful for the assistance of Dr. Wade Sigurdson of the Confocal Microscope and Flow Cytometry Facility in the School of Medicine and Biomedical Sciences, University at Buffalo.

References

Alvarez JC, Diaz C, Suarez C, Fernandez JA, Gonzalez del Rey C, Navarro A, Tolivia J. Neuronal loss in human medial vestibular nucleus. Anat Rec 1998;251:431–438. [PubMed: 9713981]

Alvarez JC, Diaz C, Suarez C, Fernandez JA, Gonzalez del Rey C, Navarro A, Tolivia J. Aging and the human vestibular nuclei: morphometric analysis. Mech Ageing Dev 2000;114:149–172. [PubMed: 10802120]

Ashley MJ, Gryfe CI, Amies A. A longitudinal study of falls in an elderly population II. Some circumstances of falling. Age Ageing 1977;6:211–220. [PubMed: 596308]

Ashwell KW, Paxinos G, Watson CR. Precerebellar and vestibular nuclei of the short-beaked echidna (Tachyglossus aculeatus). Brain Struct Funct 2007;212:209–221. [PubMed: 17717693]

Baizer J, Baker J. Immunoreactivity for SMI-32 and CAT-301 in the vestibular nuclear complex of the cat. Neurosci Abs. #652.15. 2004

Baizer J, Lima R, Witelson SF, Kigar DL, Baker JF. Immunoreactivity for calretinin defines a subdivision of the medial vestibular nucleus in the human. Neurosci Abs. # 550.10. 2006

Baizer JS, Baker JF. Immunoreactivity for calcium-binding proteins defines subregions of the vestibular nuclear complex of the cat. Exp Brain Res 2005;164:78–91. [PubMed: 15662522]

Baizer JS, Baker JF. Immunoreactivity for calretinin and calbindin in the vestibular nuclear complex of the monkey. Exp Brain Res 2006a;172:103–113. [PubMed: 16369782]

Baizer JS, Baker JF. Neurochemically defined cell columns in the nucleus prepositus hypoglossi of the cat and monkey. Brain Res 2006b;1094:127–137. [PubMed: 16701575]

Bankoul S, Neuhuber WL. A direct projection from the medial vestibular nucleus to the cervical spinal dorsal horn of the rat, as demonstrated by anterograde and retrograde tracing. Anat Embryol (Berl) 1992;185:77–85. [PubMed: 1736687]

Barmack NH, Baughman RW, Eckenstein FP. Cholinergic innervation of the cerebellum of the rat by secondary vestibular afferents. Ann N Y Acad Sci 1992a;656:566–579. [PubMed: 1376098]

Barmack NH, Baughman RW, Eckenstein FP, Shojaku H. Secondary vestibular cholinergic projection to the cerebellum of rabbit and rat as revealed by choline acetyltransferase immunohistochemistry, retrograde and orthograde tracers. J Comp Neurol 1992b;317:250–270. [PubMed: 1577999]

Belknap DB, McCrea RA. Anatomical connections of the prepositus and abducens nuclei in the squirrel monkey. J Comp Neurol 1988;268:13–28. [PubMed: 3346381]

Berman, A. The brain stem of the cat. Madison, Wisconsin: University of Wisconsin Press; 1968.

Bickford ME, Guido W, Godwin DW. Neurofilament proteins in Y-cells of the cat lateral geniculate nucleus: normal expression and alteration with visual deprivation. J Neurosci 1998;18:6549–6557. [PubMed: 9698342]

Blaszczyk JW, Prince F, Raiche M, Hebert R. Effect of ageing and vision on limb load asymmetry during quiet stance. J Biomech 2000;33:1243–1248. [PubMed: 10899333]

Bloem BR, Steijns JA, Smits-Engelsman BC. An update on falls. Curr Opin Neurol 2003;16:15–26. [PubMed: 12544853]

Brodal A, Pompeiano O. The vestibular nuclei in the cat. J Anat 1957;91:438–454. [PubMed: 13475144]

Brodal, A. The vestibular nuclei and their connections, anatomy and functional correlations, Vol. Edinburgh: Oliver and Boyd; 1962.

Büttner-Ennever, J.; Gerrits, N. Vestibular System. In: Paxinos, G.; Mai, JK., editors. The Human Nervous System. Vol. Amsterdam: Elsevier; 2004. p. 1213-1241.

Büttner-Ennever JA. Patterns of connectivity in the vestibular nuclei. Ann N Y Acad Sci 1992;656:363–378. [PubMed: 1599156]

Carleton SC, Carpenter MB. Distribution of primary vestibular fibers in the brainstem and cerebellum of the monkey. Brain Res 1984;294:281–298. [PubMed: 6200186]

Drago F, Nardo L, Rampello L, Raffaele R. Vestibular compensation in aged rats with unilateral labyrinthectomy treated with dopaminergic drugs. Pharm. Res 1996;33:135–140.

Duffy KR, Livingstone MS. Loss of neurofilament labeling in the primary visual cortex of monocularly deprived monkeys. Cereb Cortex 2005;15:1146–1154. [PubMed: 15563721]

Emmers, R.; Akert, K. A stereotaxic atlas of the brain of the squirrel monkey (*Saimiri sciureus*), Vol.. Madison: University of Wisconsin Press; 1963.

Epema AH, Gerrits NM, Voogd J. Commissural and intrinsic connections of the vestibular nuclei in the rabbit: a retrograde labeling study. Exp Brain Res 1988;71:129–146. [PubMed: 2458274]

Fuentes-Santamaria V, Stein BE, McHaffie JG. Neurofilament proteins are preferentially expressed in descending output neurons of the cat the superior colliculus: a study using SMI-32. Neuroscience 2006;138:55–68. [PubMed: 16426768]

Gerrits NM, Voogd J, Nas WS. Cerebellar and olivary projections of the external and rostral internal cuneate nuclei in the cat. Exp Brain Res 1985;57:239–255. [PubMed: 3972028]

Giardino L, Zanni M, Fernandez M, Battaglia A, Pignataro O, Calza L. Plasticity of GABA(a) system during ageing: focus on vestibular compensation and possible pharmacological intervention. Brain Res 2002;929:76–86. [PubMed: 11852033]

Heskin-Sweezie, R.; Titley, HK.; Baizer, JS.; Broussard, D. Compromised vestibular compensation in the middle-aged cat. Vancouver: Canadian Neuroscience Society; 2009.

Hof PR, Morrison JH. Neurofilament protein defines regional patterns of cortical organization in the macaque monkey visual system: a quantitative immunohistochemical analysis. J Comp Neurol 1995;352:161–186. [PubMed: 7721988]

Ikeda M, Houtani T, Ueyama T, Sugimoto T. Distribution and cerebellar projections of cholinergic and corticotropin-releasing factor-containing neurons in the caudal vestibular nuclear complex and adjacent brainstem structures. Neuroscience 1992;49:635–651. [PubMed: 1380135]

Johnsson L-G. Degenerative changes and anomalies of the vestibular system in man. Laryngoscope 1971;81:1682–1694. [PubMed: 4255919]

Jones BE, Beaudet A. Distribution of acetylcholine and catecholamine neurons in the cat brainstem: a choline acetyltransferase and tyrosine hydroxylase immunohistochemical study. J Comp Neurol 1987;261:15–32. [PubMed: 2887593]

Kalchthaler T, Bascon RA, Quintos V. Falls in the institutionalized elderly. J Am Geriatr Soc 1978;26:424–428. [PubMed: 681660]

Kevetter GA, Leonard RB, Newlands SD, Perachio AA. Central distribution of vestibular afferents that innervate the anterior or lateral semicircular canal in the mongolian gerbil. J Vestib Res 2004;14:1–15. [PubMed: 15156092]

Kimura H, McGeer PL, Peng JH, McGeer EG. The central cholinergic system studied by choline acetyltransferase immunohistochemistry in the cat. J Comp Neurol 1981;200:151–201. [PubMed: 7287919]

Korte GE. The brainstem projection of the vestibular nerve in the cat. J Comp Neurol 1979;184:279–292. [PubMed: 762285]

Koutcherov, Y.; Huang, XF.; Halliday, G.; Paxinos, G. Organization of human brainstem nuclei. In: Paxinos, G.; Mai, JK., editors. The Human Nervous System. Vol. Amsterdam: Elsevier; 2004. p. 273-321.

Ksiezak-Reding H, Dickson DW, Davies P, Yen SH. Recognition of tau epitopes by anti-neurofilament antibodies that bind to Alzheimer neurofibrillary tangles. Proc Natl Acad Sci U S A 1987;84:3410–3414. [PubMed: 2437579]

Kushiro K, Bai R, Kitajima N, Sugita-Kitajima A, Uchino Y. Properties and axonal trajectories of posterior semicircular canal nerve-activated vestibulospinal neurons. Exp Brain Res 2008;191:257–264. [PubMed: 18830591]

Ladpli R, Brodal A. Experimental studies of commissural and reticular formation projections from the vestibular nuclei in the cat. Brain Res 1968;8:65–96. [PubMed: 5650812]

Langer T, Fuchs AF, Scudder CA, Chubb MC. Afferents to the flocculus of the cerebellum in the rhesus macaque as revealed by retrograde transport of horseradish peroxidase. J Comp Neurol 1985;235:1–25. [PubMed: 3989000]

Lee VM, Otvos L Jr, Carden MJ, Hollosi M, Dietzschold B, Lazzarini RA. Identification of the major multiphosphorylation site in mammalian neurofilaments. Proc Natl Acad Sci U S A 1988;85:1998–2002. [PubMed: 2450354]

McCrea RA, Horn AK. Nucleus prepositus. Prog Brain Res 2006;151:205–230. [PubMed: 16221590]

McGibbon CA. Toward a better understanding of gait changes with age and disablement: neuromuscular adaptation. Exercise and Sports Science Reviews 2003;31:102–108.

Motts SD, Slusarczyk AS, Sowick CS, Schofield BR. Distribution of cholinergic cells in guinea pig brainstem. Neuroscience 2008;154:186–195. [PubMed: 18222049]

Paige GD. Senescence of human visual-vestibular interactions. 1. Vestibulo-ocular reflex and adaptive plasticity with aging. J Vestib Res 1992;2:133–151. [PubMed: 1342388]

Paxinos, G.; Huang, XF. Atlas of the human brainstem, Vol. San Diego: Academic Press; 1995.

Paxinos, G.; Carrive, P.; Wang, H.; Wang, P-Y. Chemoarchitectonic atlas of the rat brainstem, Vol. San Diego: Academic Press; 1999.

Paxinos, G.; Huang, XF.; Toga, AW. The rhesus monkey brain in stereotaxic coordinates, Vol. San Diego, Calif.: Academic Press; 2000.

Peterson BW, Maunz RA, Fukushima K. Properties of a new vestibulospinal projection, the caudal vestibulospinal tract. Exp Brain Res 1978;32:287–292. [PubMed: 210030]

Satoh K, Armstrong DM, Fibiger HC. A comparison of the distribution of central cholinergic neurons as demonstrated by acetylcholinesterase pharmacohistochemistry and choline acetyltransferase immunohistochemistry. Brain Res Bull 1983;11:693–720. [PubMed: 6362780]

Sekerkova G, Ilijic E, Mugnaini E, Baker JF. Otolith organ or semicircular canal stimulation induces c-fos expression in unipolar brush cells and granule cells of cat and squirrel monkey. Exp Brain Res 2005;164:286–300. [PubMed: 15940501]

Shu SY, Ju G, Fan LZ. The glucose oxidase-DAB-nickel method in peroxidase histochemistry of the nervous system. Neurosci Lett 1988;85:169–171. [PubMed: 3374833]

Somana R, Walberg F. A re-examination of the cerebellar projections from the gracile, main and external cuneate nuclei in the cat. Brain Res 1980;186:33–42. [PubMed: 7357449]

Sternberger LA, Sternberger NH. Monoclonal antibodies distinguish phosphorylated and nonphosphorylated forms of neurofilaments in situ. Proc Natl Acad Sci U S A 1983;80:6126–6130. [PubMed: 6577472]

Tian J-R, Shubayev I, Baloh RW, Demer JL. Impairments in the initial horizontal vestibulo-ocular reflex of older humans. Exp. Brain Res 2001;137:309–322. [PubMed: 11355378]

Van Der Gucht E, Youakim M, Arckens L, Hof PR, Baizer JS. Variations in the structure of the prelunate gyrus in Old World monkeys. Anat Rec A Discov Mol Cell Evol Biol. 2006

Van der Gucht E, Hof PR, Van Brussel L, Burnat K, Arckens L. Neurofilament protein and neuronal activity markers define regional architectonic parcellation in the mouse visual cortex. Cereb Cortex 2007;17:2805–2819. [PubMed: 17337746]

Xiao S, McLean J, Robertson J. Neuronal intermediate filaments and ALS: a new look at an old question. Biochim Biophys Acta 2006;1762:1001–1012. [PubMed: 17045786]

Xu Z, Cork LC, Griffin JW, Cleveland DW. Involvement of neurofilaments in motor neuron disease. J Cell Sci Suppl 1993;17:101–108. [PubMed: 8144684]

Zhang JH, Sampogna S, Morales FR, Chase MH. Age-dependent changes in the midsized neurofilament subunit in sensory-motor systems of the cat brainstem: an immunocytochemical study. J Gerontol A Biol Sci Med Sci 2000;55:B233–B241. [PubMed: 10819310]

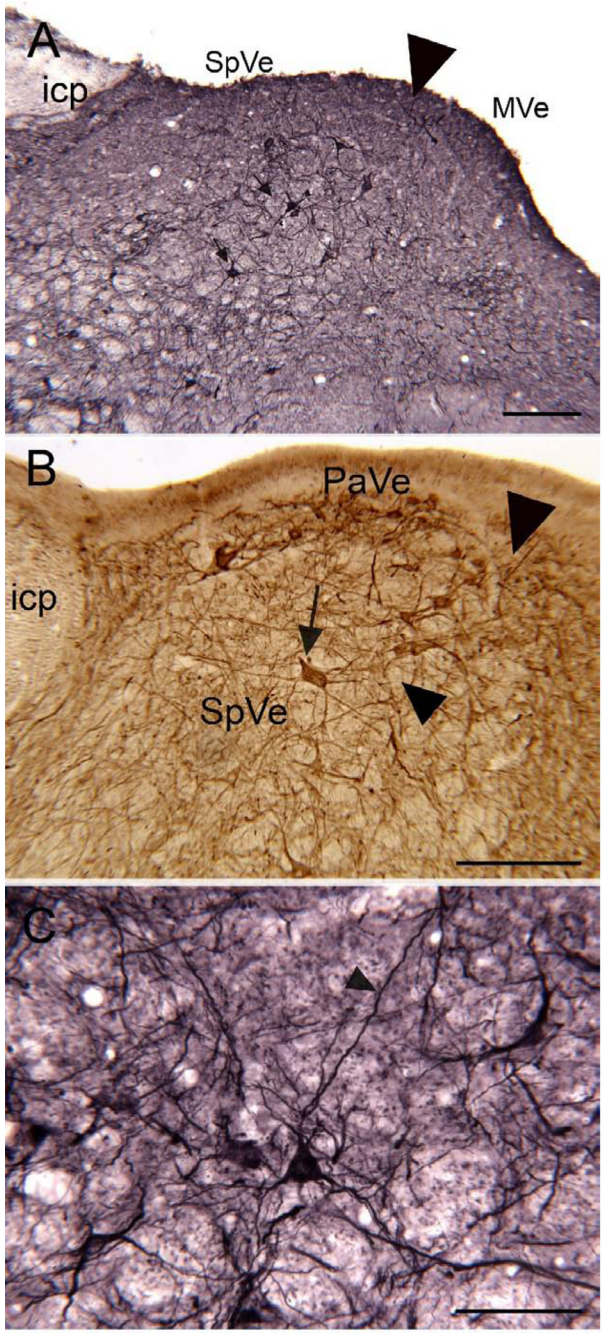

Figure 1.

SpVe. A. The arrowhead indicates the border between the MVe and the SpVe. The SpVe is crossed by stained processes running in all directions, and there are scattered large labeled cells (arrows). DAB-GO visualization. Scale bar 250 μm. icp, inferior cerebellar peduncle. **B**. Section through the SpVe at the level of the paravestibular nucleus, PaVe. Arrow s a large stained cell; arrowhead on the left indicates the locus of unstained fibers. The arrowhead on the right indicates the border with the MVe. DAB visualization. Scale bar 250 μm. **C**. Higher magnification image of a labeled cell in the SpVe with a pyramidal-shaped cell-body. DAB-GO. Scale bar 100 μm.

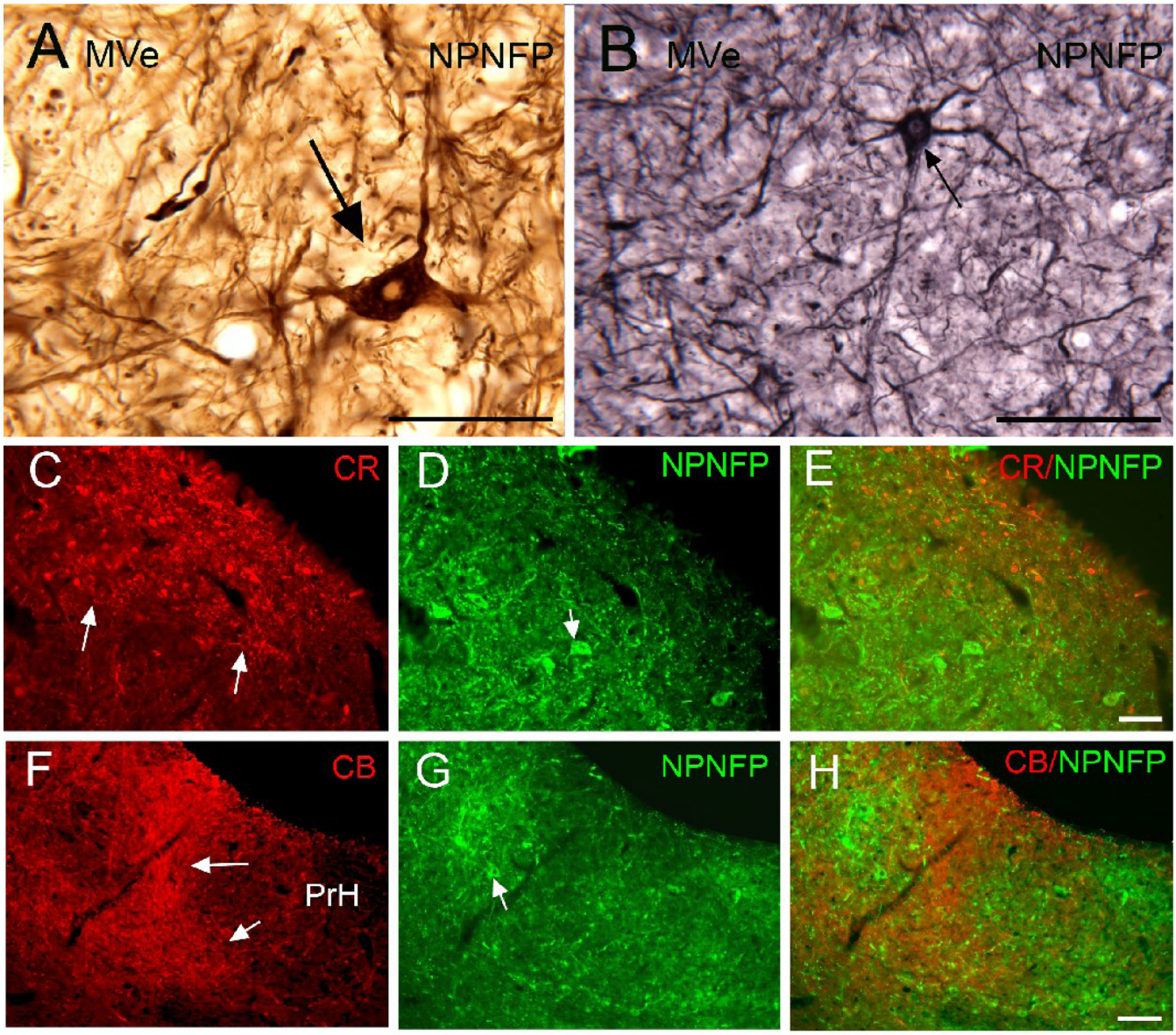

Figure 2.

MVe. A. Very large NPNFP-labeled cell, arrow, with a polygonal cell body. Note the clear nucleus. DAB. Scale bar 100 μm. **B**. Arrow shows a labeled cell with multiple stained dendrites and a pear-shaped soma. DAB-GO. Scale bar 100 μm. **C**, **D**, **E**. Comparison of the distribution of CR (C; arrows show the area of intense CR expression) and NPNFP (**D**) immunoreactivity. **E**. The merged image shows spatial separation of the two populations. Scale bar (C, D, E) 100 μm. **F**, **G**, **H**. Comparison of the distribution of CB and NPNFP immunoreactivity. **F**. The two arrows show the medial border of the region of intense CB immunoreactivty. **G**. The arrow shows an NPNFP cell **H**. The merged image shows that the NPNFP cell is lateral to the CB region. Scale bar (F,G,H) 100 μm.

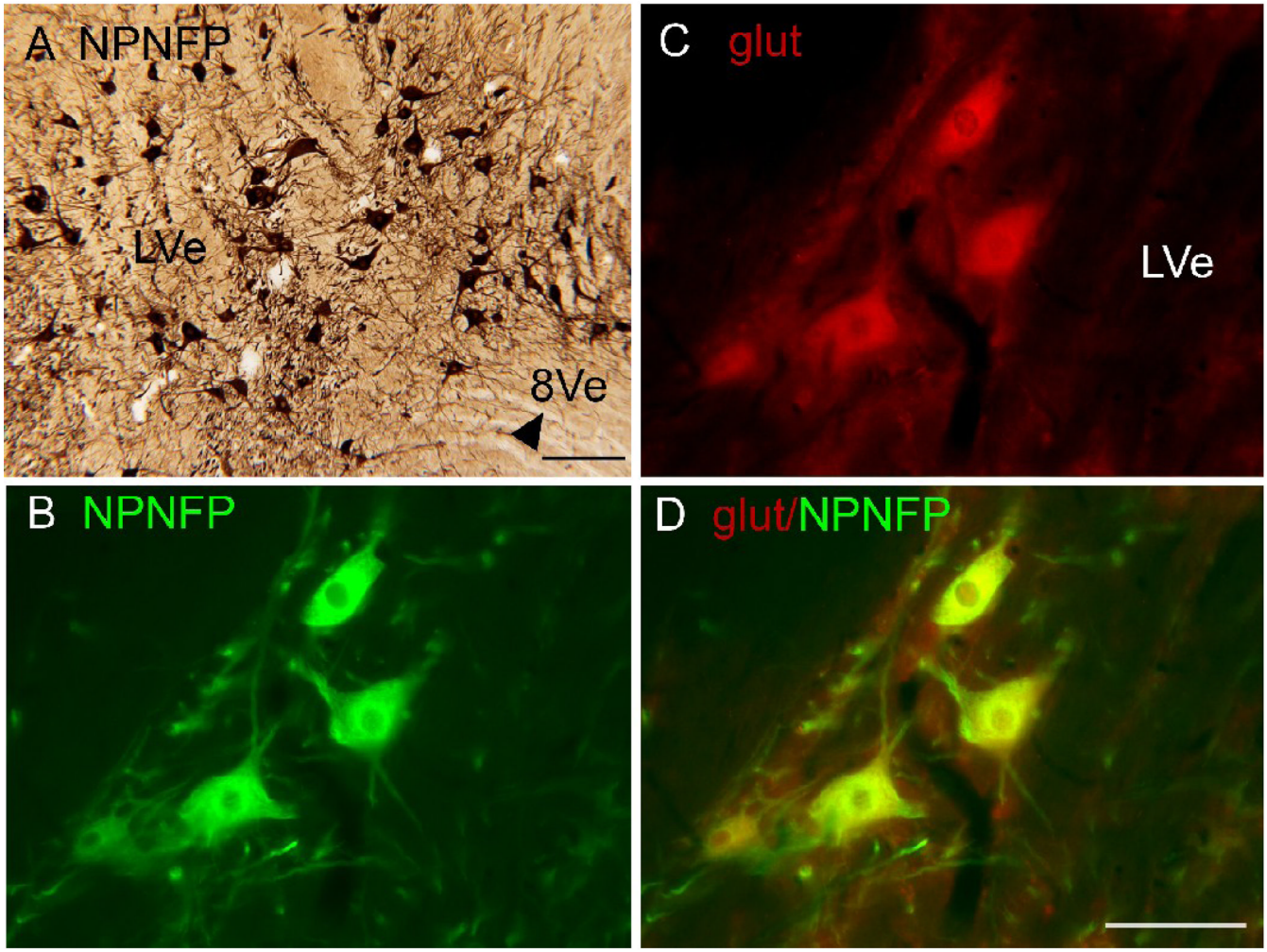

Figure 3.

A. High density of labeled large cells with a variety of soma shapes in the LVe. The arrowhead shows the unlabeled fibers of the eighth vestibular nerve (8Ve). DAB. Scale bar 250 μm. **B**. NPNFP label of three cells in the LVe. **C**. Expression of the glutamate transporter in those cells. **D**. The merged image shows colocalization of the two proteins. Scale bar 100 μm.

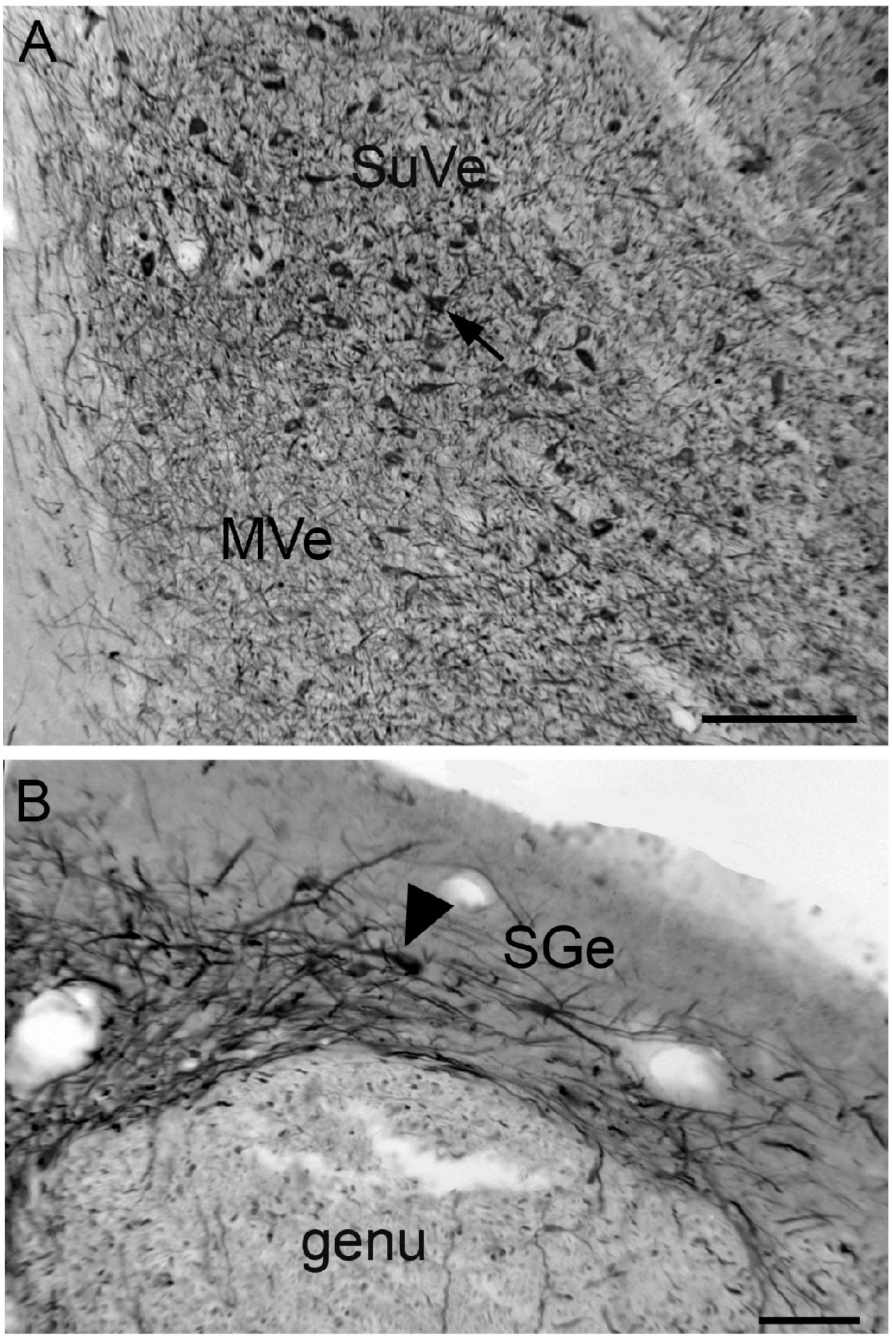

Figure 4.
A. Cells in the SuVe labeled for NPNFP. DAB. Scale bar 250 μm. **B**. Labeled cells (arrowhead) and processes in the SGe. DAB. Scale bar 100 μm.

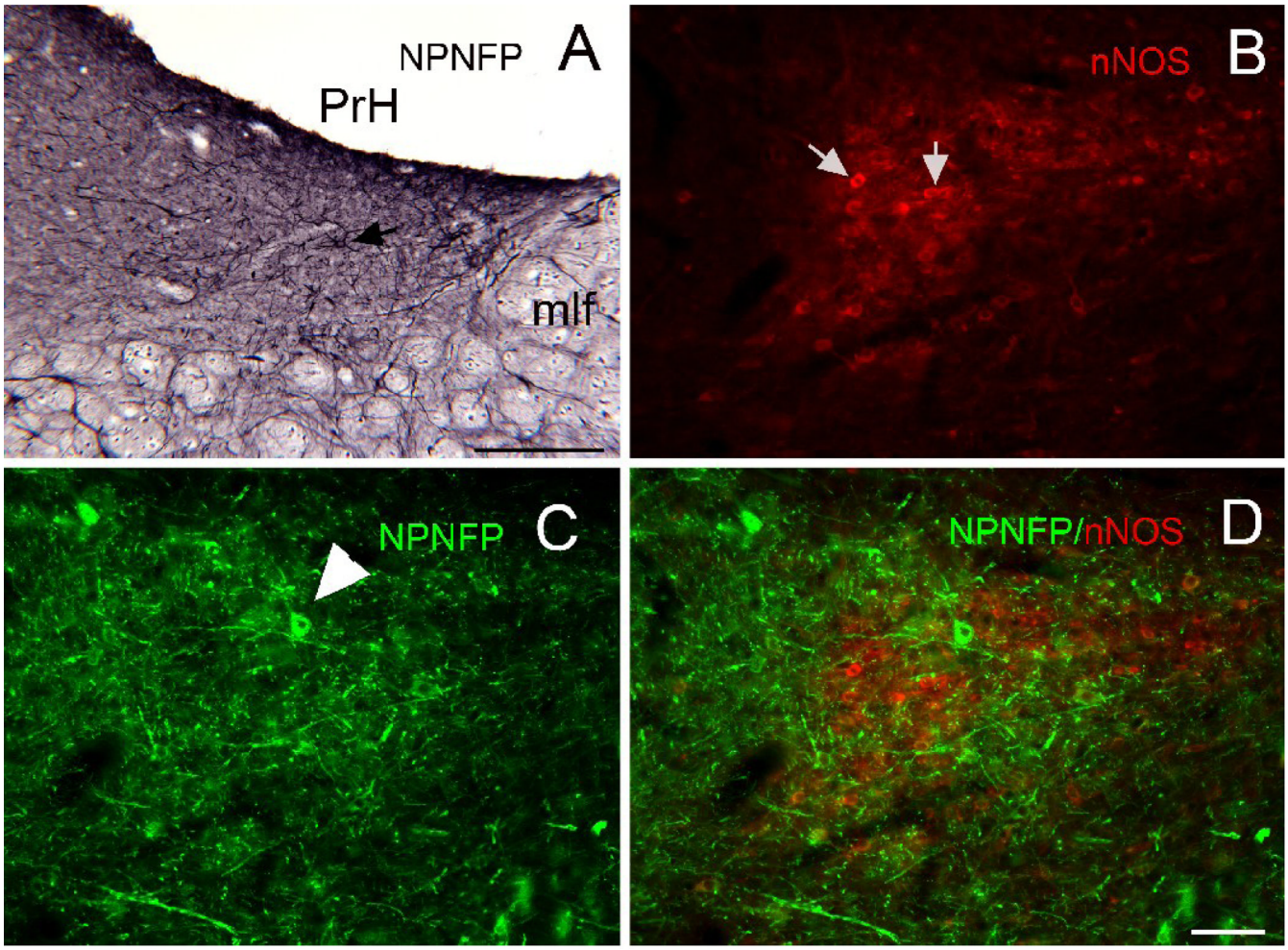

Figure 5.

A. Scattered cells (example at arrow) in PrH are labeled for NPNFP. DAB-GO. Scale bar 250 μm. mlf, medial longitudinal fasciculus. **B**. Triangular region of nNOS immunoreactivty in PrH. Arrows indicate two labeled cells. **C**. NPNFP in cells and dendrites in PrH. The arrowhead indicates a labeled cell. **D**. Merged image showing that the NPNFP cell is found within the nNOS cell cluster but does not colocalize nNOS. Scale bar 100 μm (B, C, D).

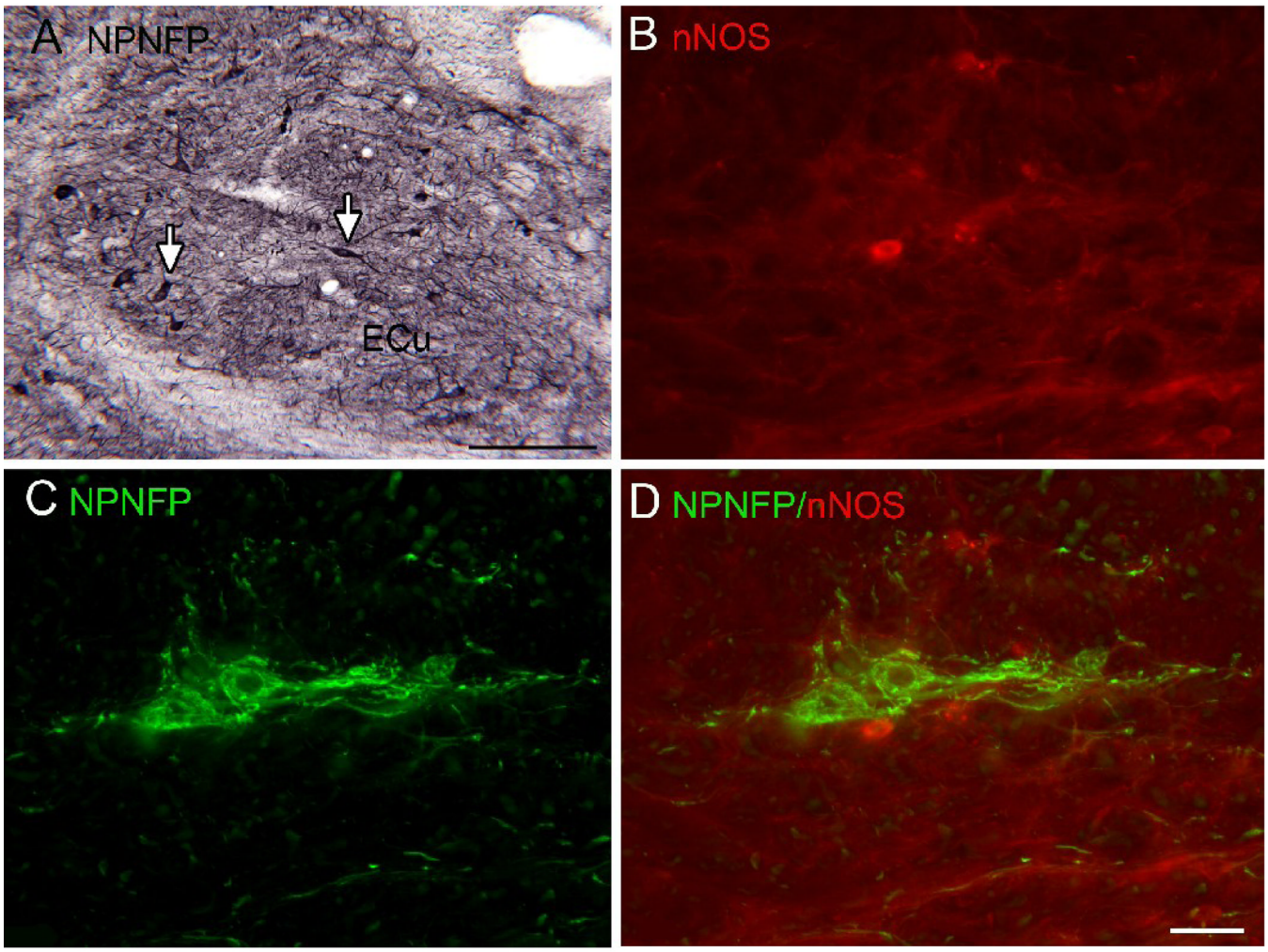

Figure 6.

A. Scattered cells and dendrites in the ECu express NPNFP; the arrows show examples of labeled cells with polygonal (left) and spindle-shaped somas (right). DAB-GO. Scale bar 250 μm. **B**. nNOS-ir cell in ECu. **C**. NPNFP label in cells in the ECu. **D**. The merged image shows expression of nNOS and NPNFP in different cells in the ECu .Scale bar 100 μm (B,C,D).

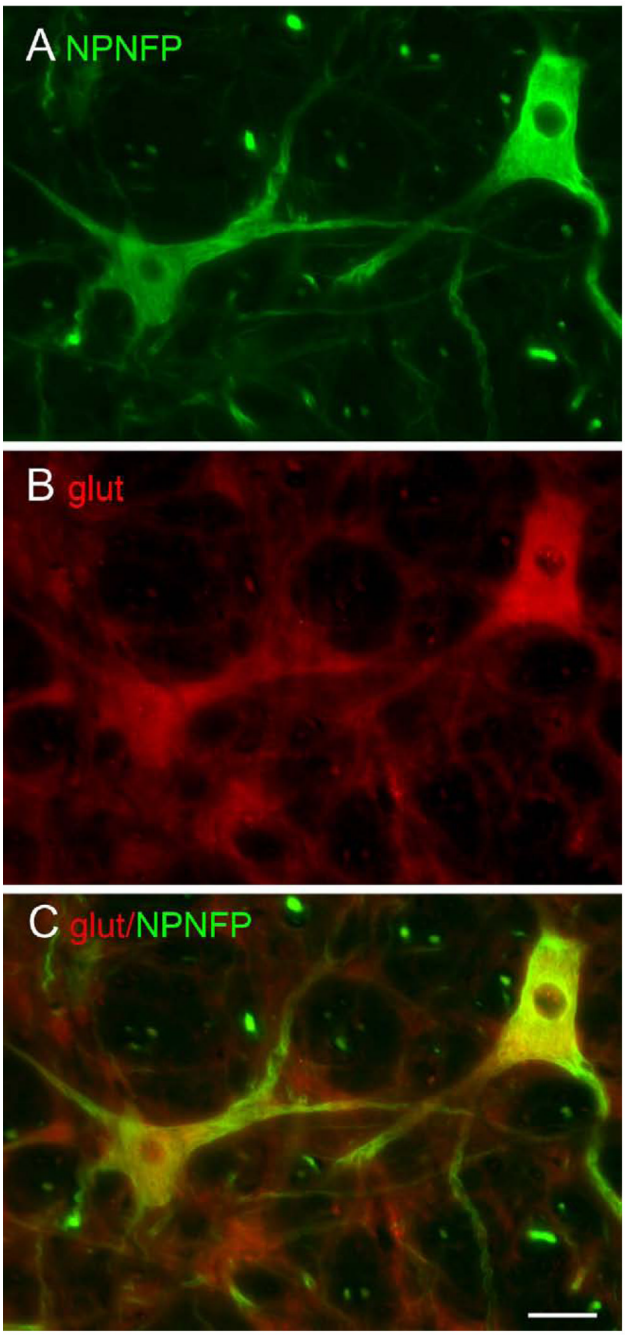

Figure 7.
A. Large NPNFP labeled cells in the RF. **B**. The same cells are labeled by an antibody to a glutamate transporter. **C**. Colocalization of the glutamate transporter and NPNFP in RF cells. Scale bar 100 μm, all panels.

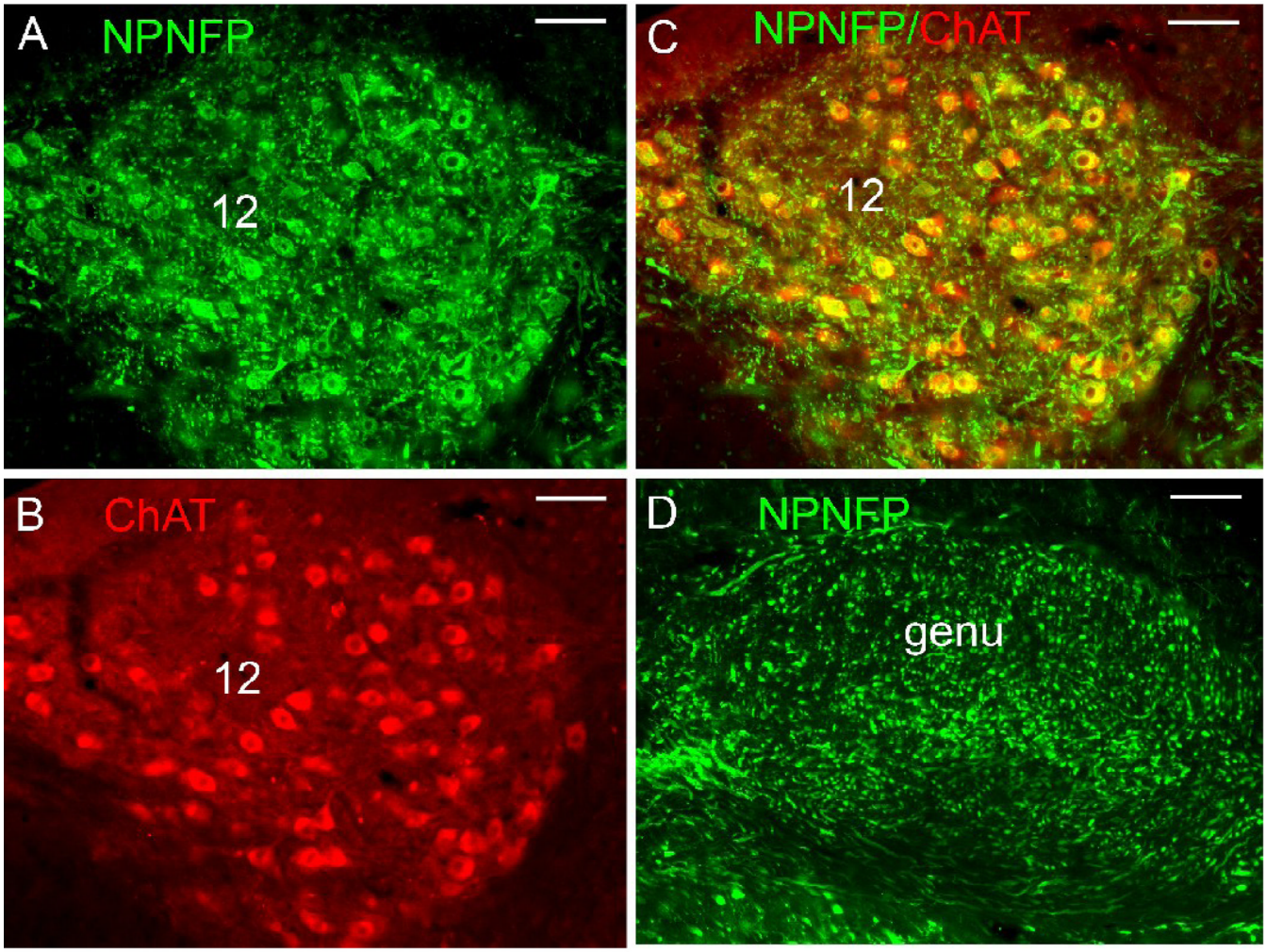

Figure 8.
NPNFP and ChAT in cranial nerve nuclei and axons. **A**. NPNFP in cells of the nucleus of the 12 cranial nerve. **B**. ChAT expression. **C**. colocalization of NPNFP and ChAT. **D**. Expression of NPNFP in the genu of the seventh nerve. Scale bars 100 μm.